Available online at www.sciencedirect.com
SCIENCE DIRECT®
Journal of Hydrology 319 (2006) 339–356
Journal of Hydrology
www.elsevier.com/locate/jhydrol

Testing nutrient flushing hypotheses at the hillslope scale: A virtual experiment approach

Markus Weiler*, Jeffrey J. McDonnell

Departments of Forest Resources Management and Geography, University of British Columbia, 2037-2424 Main Mall, Vancouver, BC, Canada V6T 1Z4

Received 4 August 2004; revised 30 June 2005; accepted 30 June 2005

Abstract

The delivery mechanisms of labile nutrients (e.g. NO_3, DON and DOC) to streams are poorly understood. Recent work has quantified the relationship between storm DOC dynamics and the connectedness of catchment units and between pre-storm wetness and transient groundwater NO_3 flushing potential. While several studies have shown N and C flushing during storm events as the important mechanism in the export of DOC and DON in small catchments, the actual mechanisms at the hillslope scale have remained equivocal. The difficulty in isolating cause and effect in field studies is made difficult due to the spatial variability of soil properties, the limited ability to detect flow pathways within the soil, and other unknowns. Some hillslopes show preferential flow behavior that may allow transmission of hillslope runoff and labile nutrients with little matrix interaction; others do not. Thus, field studies are only partially useful in equating C and N sources with water flow and transport. This paper presents a new approach to the study of hydrological controls on labile nutrient flushing at the hillslope scale. We present virtual experiments that focus on quantifying the first-order controls on flow pathways and nutrient transport in hillslopes. We define virtual experiments as numerical experiments with a model driven by collective field intelligence. We present a new distributed model that describes the lateral saturated and vertical unsaturated water flow from hypothetical finite nutrient sources in the upper soil horizons. We describe how depth distributions of transmissivity and drainable porosity, soil depth variability, as well as mass exchange between the saturated and unsaturated zone influence the mobilization, flushing and release of labile nutrients at the hillslope scale. We argue that this virtual experiment approach may provide a well-founded basis for defining the first-order controls and linkages between hydrology and biogeochemistry at the hillslope scale and perhaps form a basis for predicting flushing and transport of labile nutrients from upland to riparian zones.

Keywords: Virtual experiments; Hillslope hydrology; Nutrients; Mobilization; Flushing; Runoff generation

1. Introduction

The hydrological controls on the flushing of labile nutrients at the hillslope and headwater catchment scale are still poorly understood. Several studies have shown that stream DOC concentrations often peak on

* Corresponding author. Tel.: +1 604 822 3169; fax: +1 604 822 9106.
E-mail address: markus.weiler@ubc.ca (M. Weiler).

0022-1694/$ - see front matter © 2005 Elsevier Ltd All rights reserved.
doi:10.1016/j.jhydrol.2005.06.040

the rising limb of the snowmelt and rainfall-induced hydrographs, prior to peak discharge, followed by a rapid decrease in concentrations following rainfall cessation or melt decline (Boyer et al., 1997; Hornberger et al., 1994). Creed and Band (1998a,b) and Inamdar et al. (2004) found a similar trajectory in nitrate concentrations for both spring snowmelt and autumn rainfall events.

These and other studies have attributed the early peaks in the nutrient concentrations to the Hornberger et al. (1994) 'flushing' hypothesis, which is also based on earlier studies, for example, by Pinder and Jones (1969); Anderson and Burt (1982), whereby nutrients are leached from near-surface layers by a rising water table (Weyman, 1973) followed by a quick lateral transport of these leached nutrients to the stream via near-surface subsurface stormflow on the hillslope or surface, saturation excess runoff in the riparian zone. This rapid delivery of nutrients with surface runoff is often assumed to explain the early expression of these nutrients on the discharge hydrograph. Hydrologically, a key feature of this perceptual model is full-column saturation of the soil profile or at least water table rise high enough into the soil profile to encounter near-surface soils with high transmissivity and hence, potential for significant lateral flow to occur. This so-called transmissivity feedback is now a common hypothesis to explain lateral flushing of labile nutrients (Bishop et al., 2004). A key requirement of the 'flushing' hypothesis biogeochemically, is the ready availability of excess nutrients in the near surface soil horizons—now axiomatic of soil biogeochemical environments (Lajtha et al., 2004; Qualls and Haines, 1991) and labile nutrient concentration profiles in undisturbed environments.

Notwithstanding these gross generalities, observations of event-scale hydro-biogeochemical flushing and draining are highly complex, often contradictory from catchment to catchment and highly equivocal overall. Recent work has revealed distinct hillslope versus riparian control on DOC flushing (McGlynn and McDonnell, 2003) whereby a rainfall or antecedent wetness threshold is necessary to activate measurable hillslope contributions to streamwater DOC concentrations. Some studies have observed distinct hotspots in and around the hillslope–riparian zone interface for exfiltration of elevated DOC concentrations (Hinton et al., 1998). For nitrate, Burns et al. (1998) observed that deep groundwater flow from distinct springs controlled summer nitrate concentrations in the channel. Similarly, Hill et al. (1999); McHale et al. (2002) did not find any evidence of nitrate flushing. Hill et al. (1999) identified throughfall as the principal contributor to stream nitrate. McHale et al. (2002) found that groundwater springs, which discharged deep till groundwater, controlled the stream nitrate chemistry during events. Moreover, McHale et al. (2002) also observed nitrate peaks on the rising limb of the stream discharge hydrographs for some summer/autumn storm events, but in contrast to Creed and Band (1998b), attributed the early nitrate expression to the quick displacement of till water by infiltrating rainwater.

In terms of studies more in line with the classical flushing hypothesis, the literature is still quite uneven on cause and effect. Welsch et al. (2001) observed staggered nitrate and DOC peaks during a summer storm event—with a nitrate peak on the rising limb and a delayed DOC peak, which followed the discharge peak (Fig. 4 in Welsch et al., 2001). Following the Creed and Band (1998a,b) rationale, Welsch et al. (2001) speculated that nitrate was flushed from the hillslope but they did not present any direct evidence to support this conclusion. Brown et al. (1999) working in the same Catskill New York catchments as Welsch et al. (2001); Burns et al. (1998) reported summer DOC peaks which occurred after the peak in discharge and DOC concentrations which were greater on the recession limb than those on the hydrograph rising limb. Brown et al. (1999) were not able to explain the lag in DOC concentrations but attributed the high DOC concentrations to hillslope O-horizon soil waters. In a forested catchment in Germany, Hangen et al. (2001) also found delayed DOC contributions that occurred after peak discharge. Hangen et al. (2001) hypothesized that the delay in DOC expression was due to the time lag associated with the onset of streamflow, which displaced DOC rich waters from the hillslope to the stream via macropores.

So what can be generalized from these studies? Perhaps, it is the one-dimensional behavior that is most clear. While the biogeochemistry of DOC, DON and NO_3 is complex and different for each nutrient form, concentrations are often found to decrease markedly with depth through the soil profile

(Bishop et al., 2004; Worrall and Burt, 1999). Results of the DIRT experiments (Lajtha et al., 2004) suggest that this decrease is often exponential. At the plot scale, soil hydraulic conductivity also declines with depth and soil bulk density increases with depth. This commonality may drive the response at the plot scale. Identification of the first-order controls on the flushing behavior remains highly equivocal in the published literature. This is further exacerbated by added complexity in how processes scale from the plot to the hillslope, from the hillslope to the riparian zone and at other key ecotonal boundaries elsewhere in the catchment. Sometimes elevated DOC concentrations appear to be displaced from the riparian zone (Hinton et al., 1998). Sometimes preferential flow is argued as the control on NO_3 flushing laterally at the hillslope scale (Buttle et al., 2001).

In this paper, we argue that for progress to be made in understanding the hydrological controls on labile nutrient flushing, we need to worry less about the complexities of individual hillslopes and need to concentrate on first-order effects. We use the concept of virtual experiments (Weiler and McDonnell, 2004) in this paper as a way to filter out non-essential elements. We acknowledge that our model is an extreme simplification of both the hydrological processes and biogeochemical processes operating. Therefore, the virtual experiment is not an attempt to 'model the system' but is rather a tool to understand a phenomenon. We use the model as a learning tool and adhere to Occam's Razor, whereby the simplest explanation that can account for the phenomenon is the best explanation. In this way, the virtual experiment is therefore another research tool that can be applied to the problem, in addition to more traditional field experimental and computer modelling.

Our overall objective of this paper is to answer the question "what is the effect of hillslope shape and antecedent wetness on nutrient mobilization". Specifically, we test for planar hillslopes and for concave hillslopes (where a riparian zone exists at the slope base) and explore (1) the importance of the transmissivity feedback hypotheses in flushing nutrient in shallow soils compared to other hypotheses (e.g. preferential flow), (2) the connection between hillslope and riparian zone, and (3) the use of concentration–discharge relationship to understand nutrient mobilization processes.

2. Theory and methods

2.1. Hill-vi

We use the physically-based hillslope model Hill-Vi as the framework for performing the virtual experiments to explore the first-order controls on nutrient flushing at the hillslope scale. The basic concepts of Hill-Vi are described in detail in Weiler and McDonnell (2004). Here, we review only briefly the basic model structure and then introduce in some detail the transport modeling component that is new to this paper. The model is based on the concept that a saturated and unsaturated zone defines each grid cell, based on DEM and soil depth information. The unsaturated zone is defined by the depth from the soil surface to the water table and time variable water content. The saturated zone is defined by the depth of the water table to an impermeable soil–bedrock interface and the porosity n. Lateral subsurface flow is calculated using the Dupuit-Forchheimer assumption and is allowed to occur only within the saturated zone. Routing is based on the grid cell by grid cell approach (Wigmosta and Lettenmaier, 1999) using the water table slope as the driving force. The depth dependence of the hydraulic conductivity in the soil profile can either be described by an exponential function or by a power law function (Weiler and McDonnell, 2004).

We selected the exponential function for soil hydraulic conductivity depth dependence for these virtual experiments. While these assumptions and model implementations are similar to existing models like DHSVM (Wigmosta et al., 1994) and RHESSys (Tague and Band, 2001), we also introduced a depth function for drainable porosity—a parameter shown to be a key first-order process control on transient water table development (Weiler and McDonnell, 2004). The drainable porosity is defined by the difference in volumetric water content between the saturated water content and the water content at a soil water tension of 100 cm (approximately field capacity). Field observations show that the drainable porosity usually declines with depth due to changes in

the soil structure and macropore development and presence (see, for example, data in Ranken, 1974; Rothacher et al., 1967; Weiler, 2001; Yee and Harr, 1977). Thus, a depth function for drainable porosity n_d can be defined as

$$n_d(z) = n_0 \exp\left(-\frac{z}{b}\right) \quad (1)$$

where n_0 is the drainable porosity at the soil surface, z is the soil depth measured from the soil surface and b is a decay coefficient.

We calculate the water balance of the unsaturated zone by the precipitation input, the vertical recharge loss into the saturated zone, and the change in water content. Recharge from the unsaturated zone to the saturated zone is controlled by a power law relation of relative saturation within the unsaturated zone and the saturated hydraulic conductivity at water table depth w (measured form the soil surface) and a power law exponent (Weiler and McDonnell, 2005). The water balance of the saturated zone is defined by the recharge input from the unsaturated zone, the lateral inflow and outflow by lateral subsurface flow and the corresponding change of water table depth. Evaporation losses from the surface are neglected in this application. Since drainable porosity is not constant with depth, the water balance of the saturated zone was solved for the exponential model of the drainable porosity (Weiler and McDonnell, 2005).

Hill-Vi includes a relatively simple solute transport routine as described by Weiler and McDonnell (2005). We extend this feature in this paper for exploring the controls on nutrient flushing. We assume complete mixing within each grid cell separated for the saturated and unsaturated zone and only advective transport in and between the saturated and unsaturated zone and in and between grid cells. Field data of labile organic nutrient concentrations in undisturbed soils (e.g. forest soils) show a distinct decline with depth (e.g. DOC and DON in Swiss forest soils (Hagedorn et al., 2001), TOC in Swedish forest soils (Bishop et al., 2004)). We used this quite common experimental evidence to define a depth distribution of nutrient concentration c in soil water

$$c(z) = c_0 \exp\left(-\frac{z}{b_m}\right) \quad (2)$$

where c_0 is the nutrient concentration at the soil surface and b_m is the decay coefficient. This concentration profile defines the initial conditions and c_0 is changing, but b_m remains constant according to the solute mass in the unsaturated zone (Eq. (8)). We can calculate directly the solute mass in the unsaturated zone assuming a uniform moisture content profile depending on the concentration distribution and the water table w, defining the vertical extent of the unsaturated zone:

$$M_{un} = \theta c_0 b_m \left[1 - \exp\left(-\frac{w}{b_m}\right)\right] \quad (3)$$

When simulating water and solute flux within Hill-Vi, we assume that the shape of the concentration profile remains essentially constant (b_m= constant). The actual mass in the unsaturated and saturated zone however, changes depending on the mass flux, as calculated below. A large preponderance of experimental evidence shows that the concentration of water draining out of a zero tension lysimeter is similar to the average concentration in the unsaturated soil (Jemison and Fox, 1994; Murdoch and Stoddard, 1992). Thus, solute flux in recharge m_r depends on the average concentration in the unsaturated zone and can be determined by

$$m_r(t) = R(t)\frac{M_{un}(t)}{S_{un}(t)} \quad (4)$$

where $R(t)$ is the recharge in one grid cell at time t and S_{un} is the water storage in the unsaturated zone that is the product of the water table depth and the water content in the unsaturated zone. The solute flux in the lateral subsurface flow from one grid cell to the next is calculated in a similar fashion by multiplying the subsurface flow with the actual concentration in the saturated zone.

Weiler and McDonnell (2004) introduced a new concept to simulate the mass exchange between the saturated and unsaturated zone under a changing water table. In this paper, we further developed this concept by including the depth distribution of drainable porosity (Eq. (1)) and the depth distribution of nutrient concentration into the mass exchange calculation. Weiler and McDonnell (2004) showed that under a falling water table, solutes are transferred (Δm) from the saturated to the unsaturated zone

depending on the concentration in the saturated zone, the water table change (Δw) and the difference between total porosity and drainable porosity (that is the proportion of water that is drained by the falling water table). Since the drainable porosity is variable with depth (it was assumed to be constant in Weiler and McDonnell, 2004), we must first calculate the average drainable porosity $\bar{n}_d$ between the water table at time t and the water table in the previous time step by:

$$\bar{n}_d = \frac{n_0 b}{\Delta w(t)} \left[\exp\left(-\frac{w(t) + \Delta w(t)}{b} \right) - \exp\left(-\frac{w(t)}{b} \right) \right] \quad (5)$$

The solute transfer under a falling water table from the saturated to the unsaturated zone can then be calculated by

$$\Delta m(t) = \frac{M_{sat}(t)}{(D - w(t)) n_{eff}} \Delta w(t)(n - \bar{n}_d) \quad (6)$$

where D is the soil depth and the actual mass of solutes in the saturated zone is defined by M_{sat}, and the effective porosity by n_{eff}. The effective porosity is a common simplification describing the porosity available for fluid flow (Bear, 1972).

If the water table is rising, Weiler and McDonnell (2004) showed that the mass transfer depends on the concentration in the unsaturated zone. They assumed an average concentration in the unsaturated zone to calculate the mass exchange. However, for using the model in application to labile nutrients, we introduce a depth distribution function for nutrient concentration. To account for this distribution, we must acknowledge a clear and transparent (and simple) way to conceptualize the probable hydrobiogeochemical processes under a rising water table condition. We assume that the rising water table can only mobilize the nutrients within the depth of the water table. Thus the actual nutrient concentration at the water table defined by the exponential depth distribution determines the solute exchange

$$\Delta m(t) = \frac{M_{un}(t)}{S_{un}(t)} \exp\left(-\frac{w(t)}{b_m} \right) \Delta w(t)(n - \bar{n}_d) \quad (7)$$

We can now calculate the solute mass balances for the unsaturated and saturated zone within each grid by

$$M_{un}(t) = M_{un}(t - \Delta t) - \Delta m(t) - m_r(t) \quad (8)$$

$$M_{sat}(t) = M_{sat}(t - \Delta t) + \Delta m(t) + m_r(t) + m_{ssf}(t) \quad (9)$$

where m_{ssf} is the mass flux due to the lateral subsurface flow.

2.2. Virtual experiment design

Designing a virtual experiment requires much pre-experimental dialog and interaction between the experimentalist and the modeler. The exercise is not one of fitting parameters to an existing experimental output, but a procedure to explore first-order effects of model decisions on 'measured' response. This often follows on from intensive field campaigns where the experimentalist may have a highly complex yet quantitative view of hillslope runoff generation. The virtual experiments reported in this paper are based on the design presented below. While these experimental design criteria will no doubt change from experiment to experiment, we present these details as an example that one might conduct and in doing so, exemplify our approach for this chosen case.

2.2.1. Hillslope topography and antecedent wetness conditions

As per our stated objectives in this paper, we test the effects of hillslope shape and antecedent wetness conditions on nutrient flushing by defining two different hillslope shapes and two different antecedent wetness conditions. Since the main objective vis-à-vis hillslope shape was to explore the effect of a hillslope with and without a riparian zone, we simply define a hillslope by a straight slope profile and a hillslope with a riparian zone at the slope base by a concave slope profile, calculated by

$$z(x) = x^a \tan\beta \frac{x_{max}}{x_{max}^a} \quad (10)$$

where x is the length in direction of the slope, z the surface elevation, x_{max} is the maximum hillslope length, $\tan\beta$ is the slope, and a is the exponent defining the profile curvature. For the concave curvature $a = 2.0$; for the straight profile $a = 1.0$. The slope for both hillslopes was set to 30% and the total

length to 100 m. These values are quite typical for hillslopes in forested headwaters in the USA Pacific Northwest (e.g. the HJ Andrews Experimental Forest) and other Pacific Rim sites where we have worked (e.g. the Maimai watershed, South Island New Zealand).

In order to account for the different antecedent wetness conditions, we saturated the two different hillslopes and simulated drainage without any further rainfall input for 5 days for the 'wet antecedent condition' and for 20 days for the 'dry antecedent conditions'. This procedure created initial conditions shown in Table 1 for the four different experiments: straight slope-dry antecedent conditions, straight slope-wet antecedent conditions, concave slope-dry antecedent conditions, and concave slope-wet antecedent conditions.

2.2.2. Soil properties

One common problem of transferring the experimental results from one site to another is that either the soil properties change or the slope geometry is different. The advantage of the virtual experiment is that, for example, the hillslope geometry can remain constant but the soil properties can change and vice versa. The virtual experiment design in this paper explores only the effect of hillslope shapes and antecedent wetness conditions. Thus the soil properties were held constant from experiment to experiment. The physical soil properties used here are based on measured data from the H.J. Andrews Experimental Forest, USA (Ranken, 1974). The resulting values are for the drainable porosity at the soil surface $n_0 = 0.09$ with a shape parameter $b = 1.5$. The saturated hydraulic conductivities at the soil surface are $K_{sat} = 1.7 \times 10^{-4}$ m s^{-1}, the total and effective porosity are 30%, and the transmissivity profile was defined by an exponent of 3.0. For simplicity, we assumed the soil depth constant within the hillslope with a depth $D = 2.0$ m. The boundary condition at the upper end of the slope was set to 'no flow' and the boundary at the lower end of the slope was set to a fixed water level, imitating a constant water level in a stream.

Table 1
Initial conditions for the four virtual hillslope experiments

Hillslope shape	Antecedent conditions	Average water storage (mm)	
		Unsaturated zone	Saturated zone
Straight	Dry	192	105
	Wet	189	180
Concave	Dry	185	125
	Wet	175	205

The shape parameter ($b_m = 0.5$) for the concentration depth distribution for a nutrient like DOC was derived from data of DOC in forest soils (as reported by Hagedorn et al., 2001 and many others). In order to avoid any specification of nutrient concentrations in the soil, we set an arbitrary initial average concentration of 1.0 g/l, resulting in a $c_0 = 4.0$ g/l for the 2 m deep soil profile. The initial mass in the unsaturated and saturated zone was then calculated assuming equilibrium conditions (see also Eq. (3)). In this simplified experiment, we treat the nutrients as a conservative solute, thus ignoring production, sorption etc. We can support this rationale by focusing strictly at the event time scale. If we were to look over longer time scales, these issues would likely become important to the coupled hydrobiogeochemcial behavior.

2.2.3. Precipitation time series

To understand nutrient flushing, draining and mobilization under natural conditions, we selected a rainfall time series from a climate station in the Pacific Northwest (Eugene WSO Airport, Oregon 352709). We selected a 500 h time window (starting Oct 1st, 1984) with a total rainfall of 236 mm and five distinctive rainfall events. This time series is typical for the rainy season during fall/winter in Oregon, when frontal storms with relative low rainfall intensity are moving in from the Pacific Ocean.

3. Results

The results from the virtual experiments are divided into three sections. In the first section, we present the results from the four experiments by linking the simulated flow and concentration response at the base of the hillslope with the internal spatial–temporal response within the hillslope. These data are used to provide a general understanding of event processes. In Section 3.2, we will present

the concentration–discharge data for the same experiments. These *C–Q* plots are a well-established way in the experimental literature to analyze nutrient behavior in watersheds in relation to streamflow response (Anderson et al., 1997; Buttle et al., 2001; Evans and Davies, 1998; Hall, 1970; Lawrence and Driscoll, 1990). The last section explores more specifically the time and geographic sources of the slope base nutrient export, testing different flushing hypotheses on nutrient flux from the planar hillslope and its relation and connectedness to the hillslope–riparian zone interface.

3.1. Flow and concentration response

The simulated flow and concentration response at the base of the hillslope together with the spatial–temporal response within the hillslope for the experiment with a straight hillslope under dry antecedent soil moisture conditions (straight-dry) is shown in Fig. 1. The upper panel shows the rainfall time series together with the simulated average recharge within the slope and the lateral subsurface flow at the base of the hillslope. Recharge responds rapidly to storm rainfall, especially for the last event under the wetter soil conditions. The resulting subsurface flow is delayed relative to recharge but still shows a storm related response. This is in keeping with how we might conceptualize the sequence of conversion of vertical to lateral flow on a hillslope (Tromp-van Meerveld, 2004). The next panel shows the average concentration in recharge, subsurface flow and in the saturated and unsaturated zone. It is important to note that concentrations in the unsaturated and saturated zone change due to cell to cell import and export of nutrients and also due to volume change of the zones themselves (i.e. water table rise and fall in the saturated zone and changing water content in the unsaturated zone). The concentration response in the unsaturated zone is significant, and follows the general pattern of recharge; however, the concentration response in the subsurface flow is low by comparison and strongly lagged and damped. While average concentrations in the unsaturated zone generally decrease with time, saturated zone concentrations remain constant. The lower two panels show the spatial-temporal response internal to the hillslope: the horizontal axis shows time and the vertical axis space (i.e. horizontal distance from the base of the hillslope). The space axis is represented schematically by the depicted cross-section of the hillslope on the right side of the plot (light gray area is the soil, dark grey area is the impermeable bedrock). These 'slope diagrams' are rotated 90° to the right for ease of seeing schematically how horizontal distance equates to distance upslope.

The gray shaded regions in the time-space plots (Fig. 1) show regions between two concentrations in the vertical recharge flux (third panel) and the lateral subsurface flux (fourth panel). The dashed and dotted contours show lines of equal relative water content (1.0 = saturation) in the unsaturated zone (third panel) and lines of equal relative water table height (0.0 = at the soil–bedrock interface, 1.0 = at the soil surface). The third panel for the unsaturated zone shows relative spatially uniform water content changes, but higher concentration in the recharge in the lower part of the hillslope. In the fourth panel for the saturated zone, water table response is more related to the hillslope position and more delayed as the water content response in the unsaturated zone. The concentrations in the subsurface flow look quite similar to the concentration in the recharge. In general, the lateral subsurface stormflow and its corresponding concentration response to rain are weak and delayed.

The results for the second virtual experiment for the straight hillslope under wet antecedent soil moisture conditions (straight-wet) are shown in Fig. 2, as per the same types of diagrams for experiment 1. Not surprisingly, the recharge and subsurface flow response are much more pronounced, compared to the straight-dry experiment. The first storms under the wetter initial conditions result in a larger response. The concentration time series is also more variable compared to the straight-dry experiment, in particular for the recharge concentration. Concentration in the subsurface flow is still constant. Water content response in the unsaturated zone (third panel) is strongly dependent on the rainfall intensity. Also concentration in recharge is more dependent on time. Nevertheless, there are some concentration patterns for the first storms where the concentration in recharge is much higher, especially closer to the base of the hillslope. The water table response (fourth panel) is faster and larger compared to the

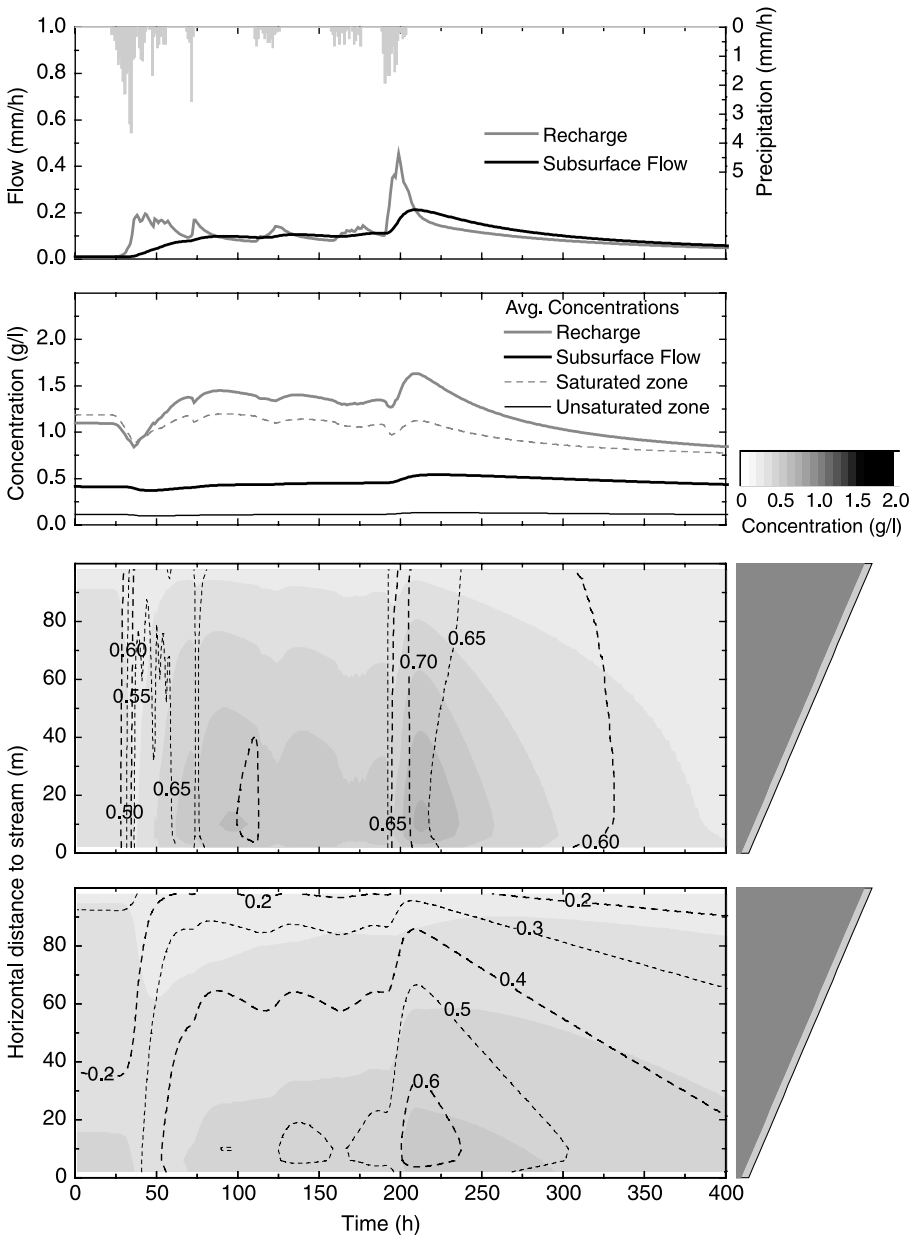

Fig. 1. Results of the virtual experiment for the straight hillslope under dry antecedent soil moisture conditions (straight-dry). The upper panel shows the rainfall time series together with the simulated average recharge within the slope and the lateral subsurface flow at the base of the hillslope. The second panel shows the average concentration in recharge, subsurface flow and in the saturated and unsaturated zone. The lower two panels show the spatial-temporal response internal to the hillslope: the horizontal axis shows time and the vertical axis space (i.e. horizontal distance from the base of the hillslope). The space axis is represented schematically by the depicted cross-section of the hillslope on the right-side of the plot (light gray area is the soil, dark grey area is the impermeable bedrock). These 'slope diagrams' are rotated 90° to the right for ease of seeing schematically how horizontal distance equates to distance upslope. The gray shaded areas in the time-space plots show areas between two concentrations in the vertical recharge flux (third panel) and the lateral subsurface flux (fourth panel). The dashed and dotted contours show lines of equal relative water content (1.0: saturation) in the unsaturated zone (third panel) and lines of equal relative water table height (0.0: at the soil–bedrock interface, 1.0: at the soil surface).

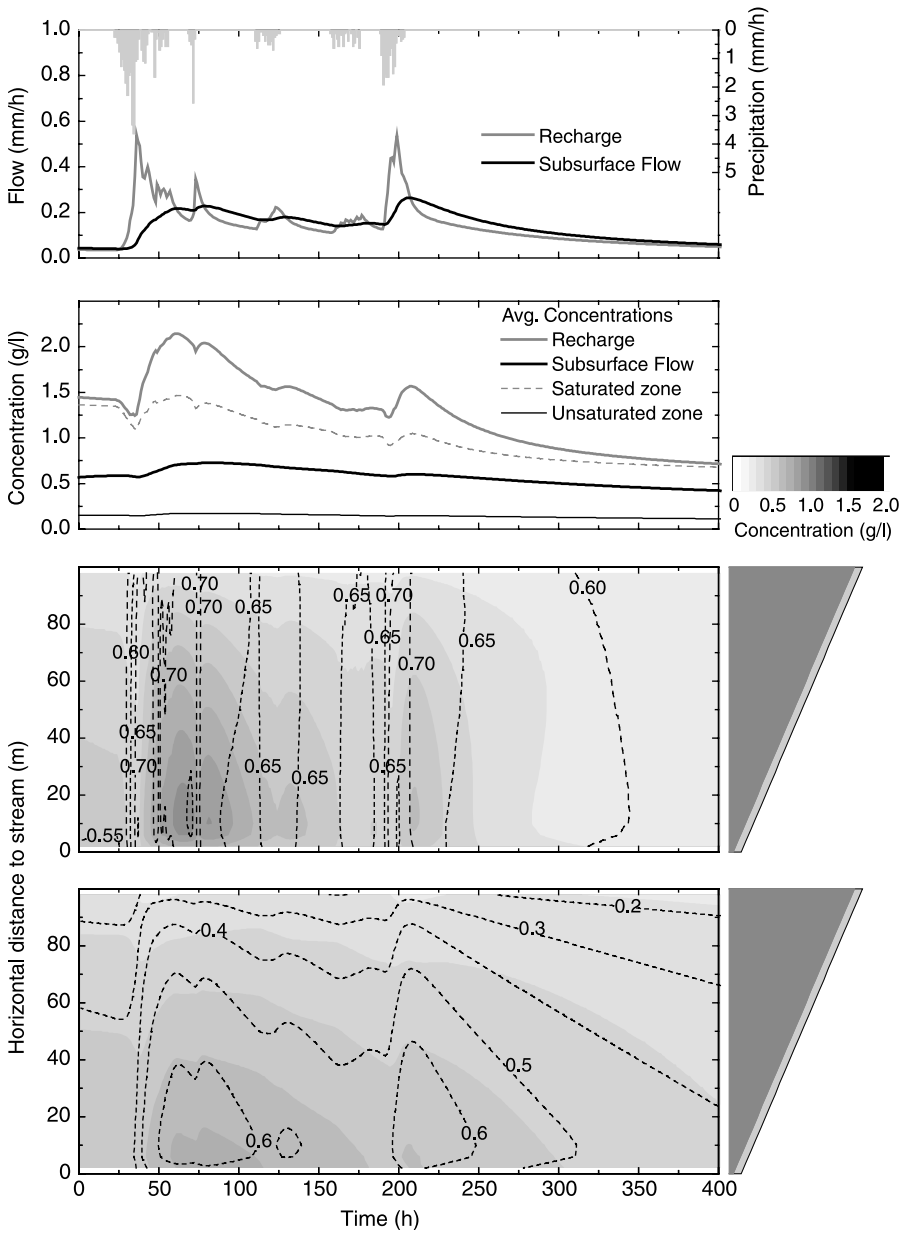

Fig. 2. Results of the virtual experiment for the straight hillslope under wet antecedent soil moisture conditions (straight-wet). The upper panel shows the rainfall time series together with the simulated average recharge within the slope and the lateral subsurface flow at the base of the hillslope. The second panel shows the average concentration in recharge, subsurface flow and in the saturated and unsaturated zone. The lower two panels show the spatial–temporal response internal to the hillslope: the horizontal axis shows time and the vertical axis space (i.e. horizontal distance from the base of the hillslope). The space axis is represented schematically by the depicted cross-section of the hillslope on the right side of the plot (light gray area is the soil, dark grey area is the impermeable bedrock). These 'slope diagrams' are rotated 90° to the right for ease of seeing schematically how horizontal distance equates to distance upslope. The gray shaded areas in the time-space plots show areas between two concentrations in the vertical recharge flux (third panel) and the lateral subsurface flux (fourth panel). The dashed and dotted contours show lines of equal relative water content (1.0: saturation) in the unsaturated zone (third panel) and lines of equal relative water table height (0.0: at the soil–bedrock interface, 1.0: at the soil surface).

straight-dry experiment. Concentration in subsurface flow is a somehow smoothed picture of the spatial–temporal concentration pattern in recharge.

The results for the experiment with a concave hillslope under dry antecedent soil moisture conditions (concave-dry) are shown in Fig. 3. The recharge and subsurface flow response in the upper panel is quite similar to the response of the straight-dry experiment. However, the concentration response is quite different compared to the straight-dry experiment with a more pronounced response of the concentration in recharge as well as a higher concentration in subsurface flow. One can observe the influence of the concave hillslope profile in the spatial-temporal plots of the lower two panels. Water content response is higher in the lower, flatter part of the hillslope than in the upper steeper part. This response appears to directly influence the concentration response in the recharge (third panel). A high concentration is observed in the lower part of the hillslope during the events, especially for the later rainfall events in the time series. These higher concentration peaks appear to control the concentration response of the subsurface flow (fourth panel). Especially for the last event in the series, high concentration of lateral subsurface flow can be seen in the lower part of the hillslope. Water table response is also higher in the lower part of the slope, analogous to a riparian zone. In general, the spatial–temporal patterns for the concave slope are more distinct and pronounced compared to the more muted temporal pattern of the straight slopes.

We show the results of the fourth experiment at a concave slope under wet antecedent soil moisture conditions in Fig. 4. The first rainfall events result in high recharge (upper panel in Fig. 4) and an associated high mobilization in the unsaturated zone and concomitant high concentration in recharge (second panel). While the lateral subsurface flow response is much more delayed compared to these 1D changes, it is high compared to the previous three experiments. In particular, the subsurface flow concentration response peak at 80 h is much higher than any of the previous observations.

The spatial–temporal plots in Fig. 4 reflect the averaged result for the hillslope. Water content response in the unsaturated zone is large for the first event and is followed by very high concentrations in recharge in the lower part of the hillslope. This high level of mobilization results in very low concentrations in recharge in the lower part of the slope later in the experiment due to the resulting depletion of the unsaturated zone tracer store. The water table response (shown in the fourth panel of Fig. 4) is rapid and pronounced—so much so that we see the lower part of the hillslope close to saturation for the first time. Coincident with this are high concentrations in the subsurface flow within the lower part of the hillslope. As per the previous experiments, slope-wide spatial variations of water table, water content and concentration responses are quite marked.

3.2. Concentration–discharge relationship

Concentration–discharge relationships (C–Q-plots) are a well established tool to analyze nutrient behavior in watersheds in relation to streamflow response (Bishop et al., 2004). We apply this method to analyze the results of the four virtual experiments. When plotting the C–Q relationships for one or several rainfall–runoff events, hysteresis is commonly observed since flow response and nutrient response are frequently out of sync. The hysteresis is commonly described by its direction of rotation: clockwise and counterclockwise. If one considers the probable hysteresis direction for the two different flushing hypotheses posed earlier in this paper, we may expect a clockwise direction for the transmissivity feedback flushing and a counterclockwise direction for the flushing by the vertical-lateral preferential flow conceptual model.

Fig. 5 shows the C–Q relationships for the four experiments. The color coding reflects time and thus the direction of the looping. For the straight-dry experiment, the relationship is quite tight and a counterclockwise loop was detected. The straight-wet experiment shows a more complex behavior: the first rainfall events produce a counterclockwise loop, followed by a very narrow loop through successive rain inputs. Notwithstanding these complexities, the overall relationship follows a clockwise loop. For the concave-dry experiment, the simulations produce a overall clockwise loop including a small clockwise loop during the last storm. The C–Q relationships is tighter compared to the straight-wet experiment, however, the reader should note that the scale of

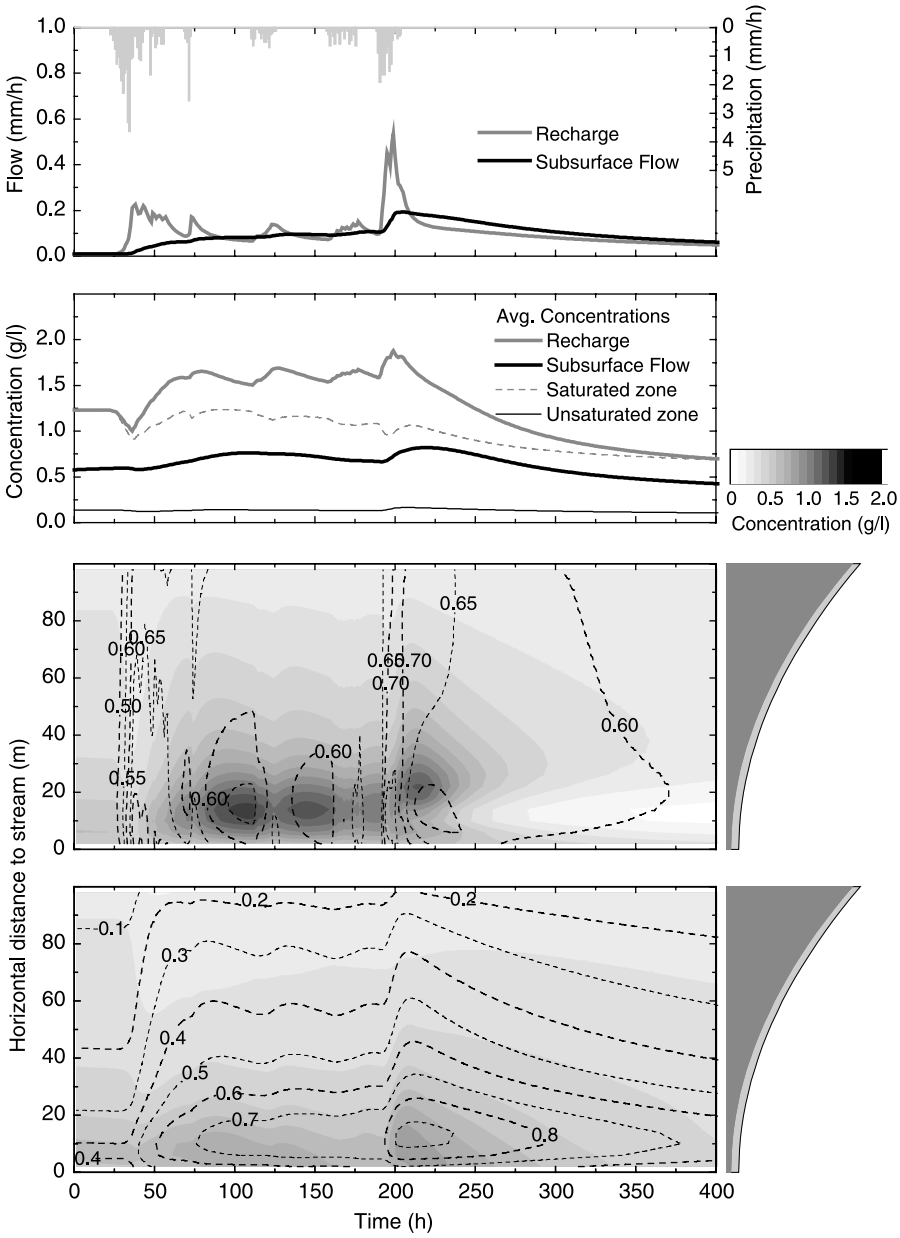

Fig. 3. Results of the virtual experiment for the concave hillslope under dry antecedent soil moisture conditions (concave-dry). The upper panel shows the rainfall time series together with the simulated average recharge within the slope and the lateral subsurface flow at the base of the hillslope. The second panel shows the average concentration in recharge, subsurface flow and in the saturated and unsaturated zone. The lower two panels show the spatial–temporal response internal to the hillslope: the horizontal axis shows time and the vertical axis space (i.e. horizontal distance from the base of the hillslope). The space axis is represented schematically by the depicted cross-section of the hillslope on the right side of the plot (light gray area is the soil, dark grey area is the impermeable bedrock). These 'slope diagrams' are rotated 90° to the right for ease of seeing schematically how horizontal distance equates to distance upslope. The gray shaded areas in the time-space plots show areas between two concentrations in the vertical recharge flux (third panel) and the lateral subsurface flux (fourth panel). The dashed and dotted contours show lines of equal relative water content (1.0: saturation) in the unsaturated zone (third panel) and lines of equal relative water table height (0.0: at the soil–bedrock interface, 1.0: at the soil surface).

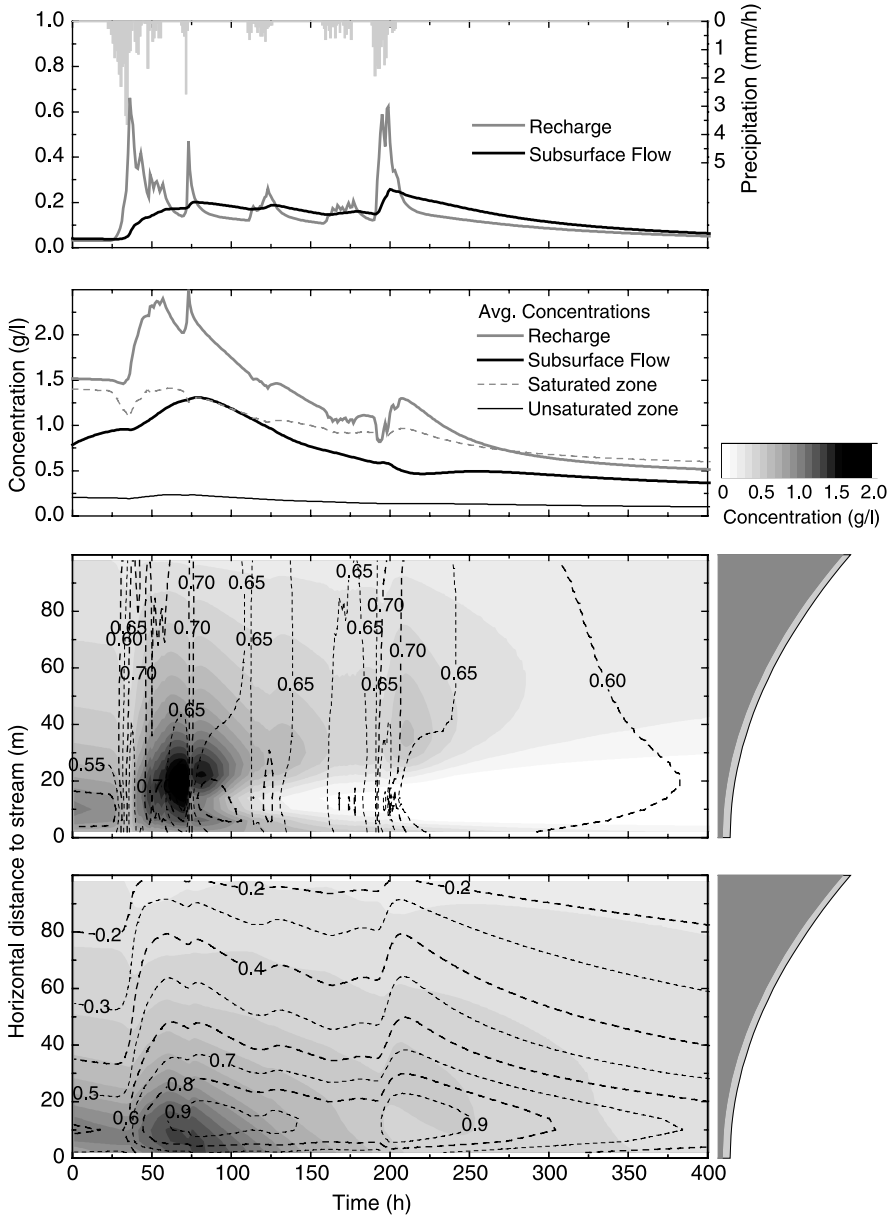

Fig. 4. Results of the virtual experiment for the concave hillslope under wet antecedent soil moisture conditions (concave-wet). The upper panel shows the rainfall time series together with the simulated average recharge within the slope and the lateral subsurface flow at the base of the hillslope. The second panel shows the average concentration in recharge, subsurface flow and in the saturated and unsaturated zone. The lower two panels show the spatial–temporal response internal to the hillslope: the horizontal axis shows time and the vertical axis space (i.e. horizontal distance from the base of the hillslope). The space axis is represented schematically by the depicted cross-section of the hillslope on the right side of the plot (light gray area is the soil, dark grey area is the impermeable bedrock). These 'slope diagrams' are rotated 90° to the right for ease of seeing schematically how horizontal distance equates to distance upslope. The gray shaded areas in the time-space plots show areas between two concentrations in the vertical recharge flux (third panel) and the lateral subsurface flux (fourth panel). The dashed and dotted contours show lines of equal relative water content (1.0: saturation) in the unsaturated zone (third panel) and lines of equal relative water table height (0.0: at the soil–bedrock interface, 1.0: at the soil surface).

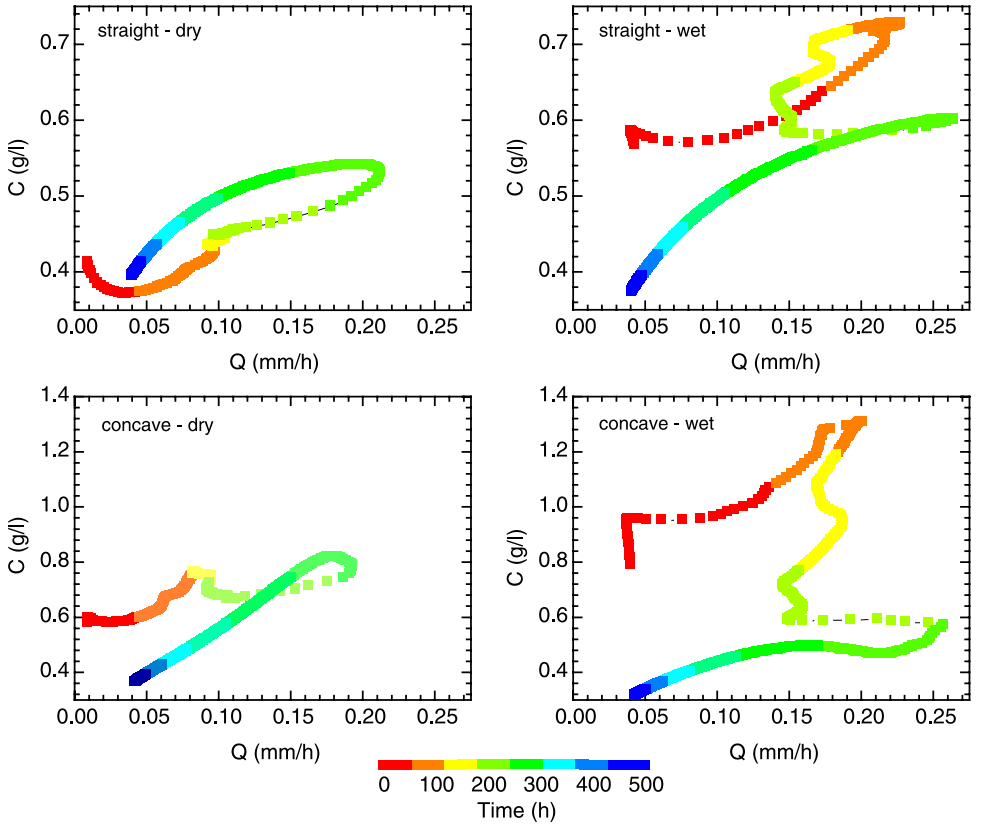

Fig. 5. Concentration–discharge plots for the four virtual experiments. Lines are color coded to show where on the hydrograph these hysteresis loops relate. Note the directional changes in looping behavior and differences in loop amplitude, as explained in the text.

the vertical axis in Fig. 5 is different to enable comparison of this experiment to the results of the concave-wet experiment. These results, shown in the lower right corner of Fig. 5, reveal a very wide clockwise hysteresis including some smaller clockwise loops.

3.3. First-order controls of nutrient export

We calculated the solute mass export mobilized by vertical flow (i.e. recharge, computed via Eq. (4)) and by water table variations (computed via Eqs. (6) and (7)). Fig. 6 shows the time series of solute export by recharge and water table variations for the four experiments. For the whole simulation period, export by recharge is higher than export by water table variations. Notwithstanding, during the first

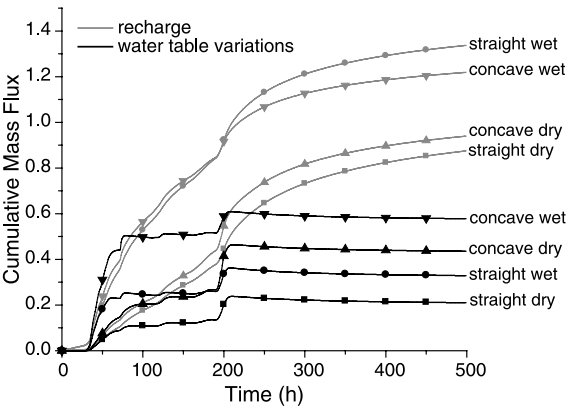

Fig. 6. Cumulative mass flux from recharge flow and water table variations for the four virtual experiments.

100 h and hence the first two major rainfall events, export by water table variations is larger for the experiments with a concave slope profile. Since recharge is a more continuous process as compared to the episodic dynamics of the water table, export by recharge is more continuous than export by water table variations. In general, the higher the water table rise (see, for example, the first event (between 40 and 70 h) for the experiments under wet initial conditions) the greater the solute export. If one ranks the export mass for the different experiments and by different mobilization processes, the experiment with wet antecedent conditions export more mass by recharge than the experiments under dry antecedent conditions. For export by water table variations, experiments for concave slope profiles show a higher total mass flux than for experiments with straight slopes.

We assess the spatial sources of mass export in our virtual experiments by defining the total amount of mobilized nutrient (i.e. mass flux) relative to the initial amount for each grid cell. This relative nutrient mobilization ratio (0.0: nothing is mobilized, 1.0: everything is mobilized) is plotted for the four experiments in Fig. 7. The shape of the mobilization ratio relative to the distance to the base of the slope differs distinctly between the straight and concave slope experiments. Mobilization for the straight slope is higher closer to the stream and decreases quite linearly for distance away from the slope base. Not surprisingly, mobilization for the concave slope experiments is much higher in the lower part of the slope (i.e. our simplistic 'riparian zone'). For both slope shapes, the mobilization ratio is always higher for the wet antecedent condition experiments. Interestingly, comparing the mobilization for the same antecedent conditions, the ratio is higher in the upper slope for the straight slope experiments.

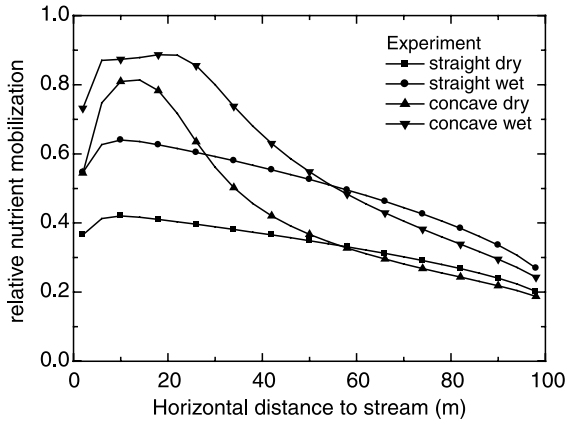

Fig. 7. Relative nutrient mobilization (0.0: nothing is mobilized, 1.0: everything is mobilized in the soil) along the hillslope transect.

4. Discussion

While several field studies have shown N and DOC flushing during storm events as the important mechanism in the export of labile nutrients in small catchments, the actual mechanisms at the hillslope scale remain equivocal. Isolating cause and effect in field studies is made difficult due to the spatial variability of soil properties, the reduced ability to detect flow pathways within the soil, and other unknowns. Some hillslopes show preferential flow behavior that may allow transmission of hillslope runoff and labile nutrients with little matrix interaction. Others show more complete mixing and lateral mobilization due to a rising water table (Creed and Band, 1998b). In between these two extremes, there are myriad possible processes and observations from field findings reported to date in the literature. We argue, that while important, field studies are only partially useful for equating DOC and N sources with water flow and transport. Our objective of this paper was to whittle down hillslope shape, soil texture and nutrient biogeochemical complexity to answer the question: 'what is the effect of hillslope shape and antecedent wetness on nutrient flushing and draining?'

The virtual experiments developed and implemented in this paper show that antecedent wetness and slope geometry exert significant control on DOC and N flushing at the hillslope scale. While the visualizations for the four experiments showed specific details and subsurface flow and concentration differences, the C–Q relations for the slope outflow suggest that the two causes of nutrient mobilization may take place simultaneously, but are more pronounced depending slope geometry and antecedent wetness. We expected characteristic loop

directions to be clockwise for the transmissivity feedback flushing process and counter-clockwise for the vertical to lateral bypass process. Our virtual experiment results suggest that the transmissivity feedback flushing process is more important for the concave slopes than for the straight slopes. Furthermore, we would conclude that the transmissivity feedback hypothesis is more important under wet than under dry antecedent moisture conditions. To test these assertions, we then analyzed for the origin of the nutrient mobilization by evaluating the influence of the two different flushing hypotheses on nutrient mass export from the hillslope. These results showed that the transmissivity feedback flushing process is more important for the concave slopes than for the straight slopes and more important under wet than under dry antecedent moisture conditions. In addition, higher mobilization for the wet antecedent conditions is supported by higher mobilization due to recharge compared to the dryer antecedent conditions.

4.1. The effect of a riparian zone

Following their hypothesis of riparian areas as source areas of nitrate, McGlynn and McDonnell (2003) further proposed that the catchment's N-flushing response would be strongly regulated by how, where, and at what rate these riparian areas function in the catchment. McGlynn and McDonnell (2003) hypothesized that the rate of change of riparian saturation and not the total riparian width would be the key determinant in a catchment's N flushing response. We found that the riparian zone (the lower part in the concave slopes) is the primary source of nutrient mobilization even though we assumed a constant initial concentration of nutrients in the hillslope. The greater flow dynamics, water table response and water content change in the riparian zone amplifies nutrient mobilization compared to a hillslope without riparian zone. Thus the rate of change of riparian saturation that we explore in our model may be a key factor as it may be a surrogate for the dynamics in the riparian zone. However, the upper slope still mobilized nutrients that are transported to the stream (for our set-up). This behavior may change when the volume of the riparian zone is larger (e.g. deeper soils, larger riparian zone width) and the mixing ratio between the hillslope water with the riparian water is larger. This is consistent with recent experimental work of Creed and Band (1998b). They showed that during a storm event, the proportion of riparian runoff was larger on the rising than falling limb of the hydrograph while the proportion of hillslope runoff was smaller on the rising than falling limb of the hydrograph. The delayed response of hillslope runoff resulted in a disconnection between hillslope and riparian areas early in the event and higher DOC concentrations on the rising limb than the falling limb of the event hydrograph. Later in the event, Creed and Band (1998b) showed that hillslope and riparian areas became connected once the hillslope soil moisture deficits were satisfied. They suggested that the relative timing of riparian and hillslope source contributions, and the connections and disconnections of dominant runoff contributing areas were the first-order catchment controls on stream DOC concentrations and mass export.

In general, the spatial distribution of riparian areas in the catchment and their connectedness with the stream network will be a key for delivery of nutrients and thus regulate the nutrient flushing response. Although Creed and Band (1998b) had observed riparian areas as nitrate sources in their catchment, they acknowledged that riparian zones could also be potential N sinks due to processes like denitrification and thus complicate the relationship between riparian area response and the catchment N flushing response (Creed et al., 1996; Worrall and Burt, 1999). These effects remain to be explored in our virtual experiments.

4.2. On the role of virtual experiments for facilitating a dialog between hydrologist and biogeochemist

We argue that rather than a systematic examination of the first-order physical hydrological controls on nutrient flushing at the hillslope and catchment scale, field hydro-biogeochemical studies have become mired in complexity. This has made it difficult to intercompare different field sites and to draw out common process behavior that may exist. Even when major hillslope experiments and excavations are undertaken to equate flushing

mechanisms with labile nutrient response and export (e.g. Buttle et al., 2001), their results are rarely transportable to other catchments. While many useful individual experimental hillslope and catchment investigations of nutrient flushing have been completed recently (Bishop et al., 2004; McGlynn and McDonnell, 2003), we still lack a quantitative framework in which to test and compare first-order controls on water and tracer mass flux at this scale.

This paper has attempted to improve conceptualization of labile nutrient flushing at the hillslope scale by quantifying the interaction between water flow pathways, source, and mixing at the hillslope scale within a virtual experiment framework. These numerical experiments with a model, driven by collective field intelligence, are fundamentally different to traditional numerical experiments since the intent is to explore first-order controls in hillslope hydrology and biogeochemical coupling where the experimentalist and modeler work together to collectively develop and analyze the results. In addition to the traditional scalar output, visualization has been a key interpretive part of the approach. As in our previous virtual experiment applications (Weiler and McDonnell, 2004), our work is motivated by frustrations that we have had personally in experiments at various hillslopes where first-order effects on flushing often seem difficult to separate from second and third order effects. The work has been further motivated by our general philosophy that hillslope models should be simple, with few 'tunable parameters', and might serve ultimately as useful hypothesis testing tools. We have shown in this paper how one can test a number of hypotheses within a virtual experimental framework to inform a new organizational structure for labile nutrient flushing at the hillslope scale.

Finally, this paper has taken a decidedly hydrocentric view of nutrient flushing. Future experiments might take a more biogeo-centric view whereby production, mineralization, etc., are examined on the timescale of events and seasonally to better understand complex biogeochmical cycling within a hydrological context. We hope that ultimately, intercomparison and classification of field experiments and development of hydrobiogeochical catchment typologies may become common—leading to new approaches in watersheds.

5. Conclusion

The delivery mechanisms of labile nutrients (e.g. NO_3, DON and DOC) to streams are poorly understood. While several studies have shown N and C flushing during storm events as the important mechanism in the export of DOC and DON in small catchments, the actual mechanisms at the hillslope scale have remained equivocal. The difficulty in isolating cause and effect in field studies is made difficult due to the spatial variability of soil properties, the reduced ability to detect flow pathways within the soil, and other unknowns. The virtual experiments described in this paper have focused on quantifying the first-order controls on flow pathways and nutrient transport in hillslopes. These virtual experiments (numerical experiments with a model driven by collective field intelligence) used a new distributed model that describes the lateral saturated and vertical unsaturated water flow from hypothetical finite and infinite nutrient sources in the upper soil horizons. We have shown how depth distributions of transmissivity and drainable porosity, soil depth variability, as well as mass exchange between the saturated and unsaturated zone influence the mobilization, flushing and release of labile nutrients at the hillslope scale. Specifically, we found that: (1) the transmissivity feedback flushing process is more important for the concave slopes than for the straight slopes, (2) transmissivity feedback is more important under wet than under dry antecedent moisture conditions and (3) the riparian zone (the lower part our virtual concave slope) is the primary source of nutrient mobilization even though we assumed a constant initial concentration of nutrients over the entire hillslope. The greater flow dynamics, water table response and water content change in the riparian zone amplifies nutrient mobilization compared to a (straight) hillslope without riparian zone. Finally, while not a replacement for field work, we argue that this new virtual experiment approach provides a well-founded basis for defining the first-order controls and linkages between hydrology and biogeochemistry at the hillslope scale.

References

Anderson, M.G., Burt, T.P., 1982. The contribution of throughflow to storm runoff: an evaluation of a chemical mixing model. Earth Surface Processes and Landforms 33 (1), 211–225.

Anderson, S.P., Dietrich, W.E., Torres, R., Montgomery, D.R., Loague, K., 1997. Concentration-discharge relationships in runoff from a steep, unchanneled catchment. Water Resources Research 33 (1), 211–225.

Bear, J., 1972. Dynamics of Fluids in Porous Media. American Elsevier Pub. Co., New York p. 764.

Bishop, K., Seibert, J., Köhler, S., Laudon, H., 2004. Resolving the double paradox of rapidly mobilized old water with highly variable responses in runoff chemistry. Hydrological Processes 18 (1), 185–189.

Boyer, E.W., Hornberger, G.M., Bencala, K.E., McKnight, D.M., 1997. Response characteristics of DOC flushing in an alpine catchment. Hydrological Processes 11 (12), 1635–1647.

Brown, V.A., McDonnell, J.J., Burns, D.A., Kendall, C., 1999. The role of event water, a rapid shallow flow component, and catchment size in summer stormflow. Journal of Hydrology 217, 171–190.

Burns, D.A., et al., 1998. Base cation concentrations in subsurface flow from a forested hillsope: the role of flushing frequency. Water Resources Research 34 (12), 3535–3544.

Buttle, J.M., Lister, S.W., Hill, A.R., 2001. Controls on runoff components on a forested slope and implications for N transport. Hydrological Processes 15, 1065–1070.

Creed, I.F., Band, L.E., 1998a. Exploring functional similarity in the export of nitrate-N from forested catchments: a mechanistic modeling approach. Water Resources Research 34 (11), 3079–3093.

Creed, I.F., Band, L.E., 1998b. Export of nitrogen from catchments within a temperate forest: evidence for a unifying mechanism regulated by variable source area dynamics. Water Resources Research 34 (11), 3105–3120.

Creed, I.F., et al., 1996. Regulation of nitrate-N release from temperate forests: a test of the N flushing hypothesis. Water Resouces Research 32, 3337–3354.

Evans, C., Davies, T.D., 1998. Causes of concentration/discharge hysteresis and its potential as a tool for analysis of episode hydrochemistry. Water Resources Research 34 (1), 129–137.

Hagedorn, F., Bucher, J.B., Schleppi, P., 2001. Contrasting dynamics of dissolved inorganic and organic nitrogen in soil and surface waters of forested catchments with gleysols. Geoderma 100, 173–192.

Hall, F.R., 1970. Dissolved solids-discharge relationships. Water Resources Research 6 (3), 845–850.

Hangen, E., Lindenlaub, M., Leibundgut, C., von Wilpert, K., 2001. Investigating mechanisms of stormflow generation by natural tracers and hydrometric data: a small catchment study in the Black Forest, Germany. Hydrological Processes 15, 183–199.

Hill, A.R., Kemp, W.A., Buttle, J.M., Goodyear, D., 1999. Nitrogen chemistry of subsurface storm runoff on forested canadian shield hillslopes. Water Resources Research 35, 811–821.

Hinton, M.J., Schiff, S.L., English, M.C., 1998. Sources and flowpaths of dissolved organic carbon during storms in two forested watersheds of the precambrian shield. Biogeochemistry 41, 175–197.

Hornberger, G.M., Bencala, K.E., McKnight, D.M., 1994. Hydrological controls on dissolved organic carbon during snowmelt in the Snake River near Montezuma, Colorado. Biogeochemistry 25 (3), 147–165.

Inamdar, S.P., Christopher, S. and Mitchell, M.J., 2004. Flushing of DOC and nitrate from a forested catchment: Role of hydrologic flow paths and water sources. Hydrological Processes 18, 2651–2661.

Jemison Jr.., J.M., Fox, R.H., 1994. Nitrate leaching from nitrogen-fertilized and manured corn measured with zero-tension pan lysimeters. Journal of Environmental Quality 23 (2).

Lajtha, K. et al., 2004. Detrital controls on SOM dynamics and soil solution chemistry: an experimental approach. Geoderma, in press

Lawrence, G.B., Driscoll, C.T., 1990. Longitudinal patterns of concentration-discharge relationships in stream water draining the hubbard brook experimental forest. Journal of Hydrology 116, 147–165.

McGlynn, B.L., McDonnell, J.J., 2003. Role of discrete landscape units in controlling catchment dissolved organic carbon dynamics. Water Resources Research 39 (4). 10.1029/2002WR001525.

McHale, M.R., McDonnell, J.J., Mitchell, M.J., Cirmo, C.P., 2002. A field-based study of soil water and groundwater nitrate release in an adirondack forested watershed. Water Resouces Research 38 (4). 10.1029/2000WR000102.

Murdoch, P.S., Stoddard, J.L., 1992. The role of nitrate in the acidification of streams in the Catskill Mountains of New York. Water Resouces Research 28 (10), 2707–2720.

Pinder, G.F., Jones, J.F., 1969. Determination of the ground-water component of peak discharge from the chemistry of total runoff. Water Resources Research 5 (2), 438–445.

Qualls, R.G., Haines, B.L., 1991. Geochemistry of dissolved organic nutrients in water percolating through a forest ecosystem. Soil Science Society of American Journal 55, 1112–1123.

Ranken, D.W., 1974. Hydrologic properties of soil and subsoil on a steep, forested slope. M.S. Thesis, Oregon State University, Corvallis, p.114.

Rothacher, J., Dyrness, C.T. and Fredriksen, R.L., 1967. Hydrologic and related characteristics of three small watersheds in the Oregon Cascades, U.S. Department of Agriculture, Forest Service, Pacific Northwest Forest and Range Experiment Station, Portland, OR.

Tague, C.L., Band, L.E., 2001. Evaluating explicit and implicit routing for watershed hydro-ecological models of forest hydrology at the small catchment scale. Hydrological Processes 15, 1415–1440.

Tromp-van Meerveld, H.J., 2004. Hillslope hydrology: From patterns to processes. Ph. D. dissertation, Oregon State University, Corvallis, 270 pp.

Weiler, M., 2001. Mechanisms controlling macropore flow during infiltration—dye tracer experiments and simulations. ETHZ, ürich, Switzerland p. 151.

Weiler, M., McDonnell, J.J., 2004. Virtual experiments: a new approach for improving process conceptualization in hillslope hydrology. Journal of Hydrology 285, 3–18.

Weiler, M. and McDonnell, J.J., 2005. Virtual isotope hydrograph separation: Examining the effects of pre-event water variability on estimated runoff components. Journal of Hydrology, in review.

Welsch, D.L., Kroll, C.N., McDonnell, J.J., Burns, D.A., 2001. Topographic controls on the chemistry of subsurface stormflow. Hydrological Processes 15, 1925–1938.

Weyman, D.R., 1973. Measurements of the downslope flow of water in a soil. Journal of Hydrology 20, 267–288.

Wigmosta, M.S., Lettenmaier, D.P., 1999. A comparison of simplified methods for routing topographically driven subsurface flow. Water Resources Research 35, 255–264.

Wigmosta, M.S., Vail, L.W., Lettenmaier, D.P., 1994. A distributed hydrology-vegetation model for complex terrain. Water Resources Research 30 (6), 1665–1679.

Worrall, F., Burt, T.P., 1999. The impact of land-use change on water quality at the catchment scale: the use of export coefficient and structural models. Journal of Hydrology 221 (1–2), 75–90.

Yee, C.S., Harr, R.D., 1977. Influence of soil aggregation on slope stability in the oregon coast ranges. Environmental Geology and Water Sciences 1 (6), 367–377.